Article

Not peer-reviewed version

Facile Synthesis of Ag/ZnO Nano composites Using Fruit Peels and their Possible Applications

Shamroza Mubarik * , Aisha Nawab , Marryam Imran , Aqeela Shaheen , Ambreen Kalsoom

Posted Date: 17 December 2024

doi: 10.20944/preprints202412.1337.v1

Keywords: Adsorption; Ag/ZnO nanocomposites; Eosin Y; Cong-Red; Kinetic models

 doi:10.20944/preprints202412.1337.v1

Article

Facile Synthesis of Ag/ZnO Nano composites Using Fruit Peels and Their Possible Applications

Shamroza Mubarik[1,*], Aisha Nawab[1], Marryam Imran[1], Aqeela Shaheen[1], Ambreen Kalsoom[2]

1 Department of Chemistry, Government Sadiq College Women University, Bahawalpur, 63100, Pakistan
2 Department of Physics, Government Sadiq College Women University, Bahawalpur, 63100, Pakistan;
* Correspondence: shamroza.mubarik@gscwu.edu.pk

Abstract: This research work describes the synthesis of Ag-ZnO nanocomposites by combustion method using citrus clementina peels as an effective adsorbent material for removal of dyes. Water is an essential element for life. However, critical environmental issue of 20th century is water scarcity. Water has a wide-ranging effect on all aspects of human life, a serious hazard to public health and stability of food chain. Due to human activities the waste from our industrial, agricultural, and daily activities frequently pollutes the water. Therefore, there is an urgent need to develop cost effective and sustainable technologies for the removal of contaminants from waste water. The synthesized nanocomposites were characterized by (FTIR), UV Visible, (XRD) and (SEM). Then tested their potential toward efficient removal of Eosin Y and Congo-Red from waste water by using cost effective Adsorption method. Different parameters i.e., Dosage, Time, Concentration, PH and temperature have been studied. During Linear adsorption isotherm Langmuir and Temkin isotherms are best fitted on the adsorption of Dyes. Thermodynamic and kinetic studies have also done, while Pseudo 2nd order kinetic model showed better agreement as compared with other kinetic models. Thus synthesized Ag-ZnO Nanocomposites confirmed as excellent adsorbent material for waste water treatment.

Keywords: Adsorption; Ag/ZnO nanocomposites; Eosin Y; Cong-Red; Kinetic models

1. Introduction

The previous ten years have seen great growth in the field of nanotechnology, which is anticipated to continue in future[1]. Nanotechnology tools and techniques, which explore and fine-tune the properties, responses, and functionalities of living and non-living matter, at sizes less than 100 nm, are used to create and control novel nano- and biomaterials, as well as nano devices. The ongoing revolution in nanotechnology will lead to the creation of nanomaterials with qualities and capabilities that will improve the lives of our population, whether in the fields of health, the environment, electronics, or any other[2]. Carbon nanocomposites normally display excellent performance in adsorbing pollutants from aqueous solutions and thus increasing the usage of nanotechnology in waste water treatment is of great importance[3]. Nanocomposites are used extensively in numerous areas including life sciences, pharmaceuticals and the treatment of waste water. Nanocomposites full with metal nanoparticles are extremely effective for wastewater treatment and have antimicrobial activities[4]. Gaining a fundamental knowledge of the electrical, optical, magnetic, and mechanical characteristics of nanostructures has emerged as a multidisciplinary topic in nanotechnology, with the potential to produce the next generation of functional materials with a wide range of uses.[5]. Ag-doped ZnO nanocomposites are successfully made using a straightforward, efficient, high-yield, and inexpensive mechanochemical combustion method.[6]. Pollution is a major issue that affects the environment in varying degrees and poses a serious threat to humans and other living things, especially marine life. Water is significantly impacted by water pollution. The release of pollutants that cause water pollution, such as organic and inorganic chemicals, dyes, medicinal compounds, pathogens, and radioactive compounds, is encouraged by industrial discharges, structural improvements, and other associated anthropogenic

 doi:10.20944/preprints202412.1337.v1

activities.[7]. Point sources from businesses and municipalities represent the most risk to the quality of the water. Agriculture, urban growth, and mining all have an impact on the quality of the water. Nutrients, sediments, and hazardous substances are other non-point sources of pollution. A constant inspection of water resource policy is now required to address the issue of water pollution, which has spread to be a worldwide issue [8]. Organic and inorganic contaminants predominate in wastewater from the chemical industry. These toxins are poisonous, mutagenic, carcinogenic, and largely non-biodegradable.[9]. Dyes and pigments are major environmental pollutants used in various industries including textile, plastics, pulp and paper, leather tanning and hair coloring. Given that pigments and synthetic dyes are not biodegradable and persist in the environment for a long time, removing dye from such effluent is a difficult operation. There are several techniques, including as photocatalysis, adsorption, electrochemical precipitation, and reverse osmosis, for eliminating metal ions and dyes. However, among these methods, adsorption is low cost, effective and easy to access [10]. The goal of the current study was to adsorb eosin Y and congo-red, a model anionic dye, from an aqueous solution using nanoparticles [11] . Congo Red (diazo dye), which has an aromatic amine in its composition, is known to be carcinogenic. Azo dyes are resistant to natural deterioration due to the presence of aromatic structures. A variety of techniques, including adsorption, coagulation-flocculation, ultrasonic irradiation, ion exchange, mineralization, and photocatalysis, have been suggested to remove Congo Red from contaminated water.[12]. Eosin Y has long been used as a textile and fine art dye, and it is currently widely employed in the field of pharmaceutical preparation detection. Human activity releases the very hazardous substance eosin Y into the environment, endangering not just aquatic life but also human health. The most practical, efficient, and affordable way for eliminating organic dyes from water is adsorption; other traditional physical, chemical, and biological techniques include membrane filtration, coagulation, adsorption, photodegradation, chemical oxidation, and biological treatment. [13] Adsorption is a common technique used to cleanse industrial wastewater to get rid of organic and inorganic pollutants. Adsorption has advantages over other technologies due to its simple design, possibility for low initial investment, and lack of space requirements.[14] Adsorption is frequently recognised as a trustworthy and cost-effective wastewater treatment method. The efficiency of adsorption's removal can approach 99.9%[15]. To understand the adsorption mechanism, data from adsorption models, thermodynamics and kinetic models were also examined.

2. Material and Method

2.1. General

Eosin Y (EY MW 691.86), Congo - Red (CR MW 696.86), Silver nitrate, Zinc Hexahydrate, NaOH and HCL were taken from chemical store of GSCWU Bahawalpur. All the chemicals and reagents were of analytical grade, and used as received without further purification. Deionized water was used in synthesis of Nanocomposites while Distilled water was used in all adsorption experiments.

2.2. Synthesis of Nanocomposites

Ag-ZnO Nanocomposites were synthesized by using simple, cost effective combustion method. Citrus clementina fruits were collected from a Home Garden in Bahawalpur Punjab Pakistan. Fruits completely washed with distilled water and then dry. Peel off fruits, then peels are washed and shade dried for almost 7 days. Dried peels were grined with pistle motar to form fine powder. 5.752g of fruit powered and 2.352g Zn(NO3) is weighed on weighing balance and taken in beaker. In a separate beaker make 8% Ag(NO3) solution and add fruit poweder and Zn(NO3) in Ag (NO3) solution beaker. Heat and stirrer the solution on hot plate for 10 min at 80° C and then centrifuged. After centrifugation above solution(filtrate) taken in separate beaker for UV purpose and solid particle at the bottom washed with deionized water. These solid particles dried in vaccum oven. Dried solid particle taken in crucible and place in a muffle furnace at 500°C for 10 min. Ag doped Zn oxide nanocomposite is synthesized. Prepared nanocomposites were store in glass viols for further usage.

 doi:10.20944/preprints202412.1337.v1

Fig.1. shows the synthesis procedure of Ag- ZnO Nanocomposites from citrus clementina.

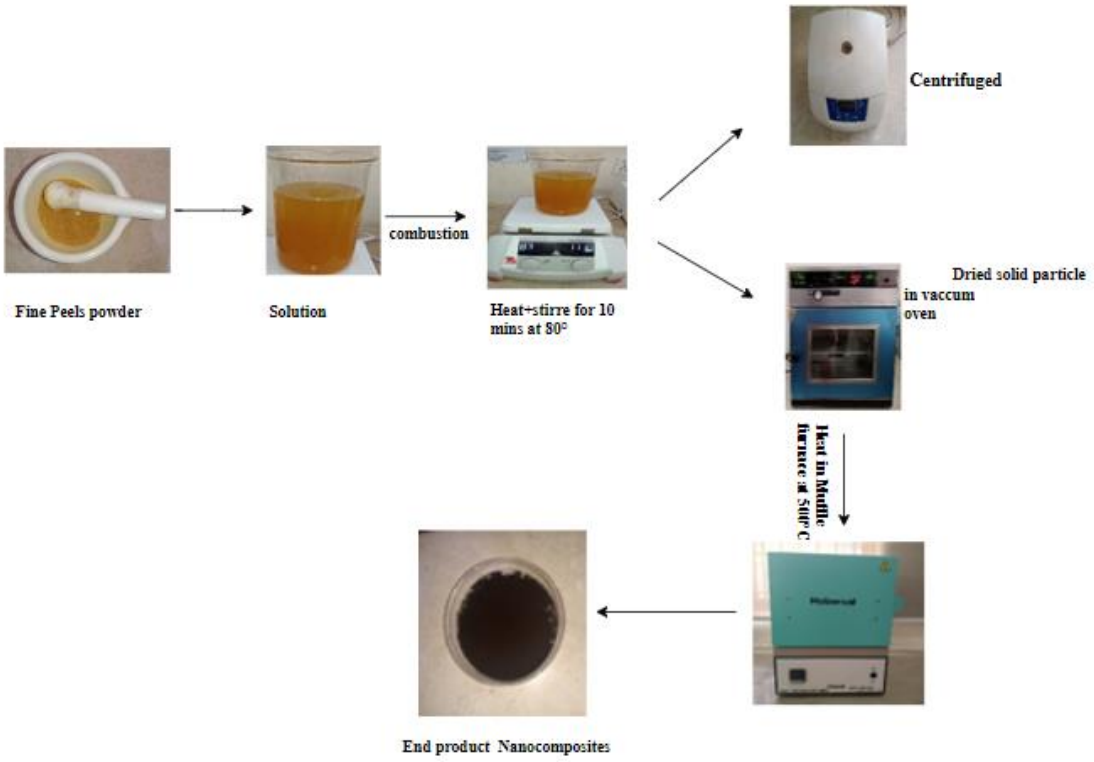

Figure 1. Green Synthesis of Nanocomposites from Citrus Peels.

2.3. Characterization of NCs

The synthesized Ag-ZnO Nanocomposites were analyzed by Uv Visible spectroscopy, FTIR spectroscopy, SEM and X- ray diffraction.

 doi:10.20944/preprints202412.1337.v1

2.3.1. UV-Visible Spectroscopy

Uv visible spectroscopy can be used to analyse a compound's optical characterizations[16]. The solution was subjected for UV–visible measurements. The spectra tell characteristic absorption peaks of ZnO at wavelength of 370 nm which can be assigned to the intrinsic band-gap absorption of ZnO due to the electron transitions from the valence band to the conduction band[17].

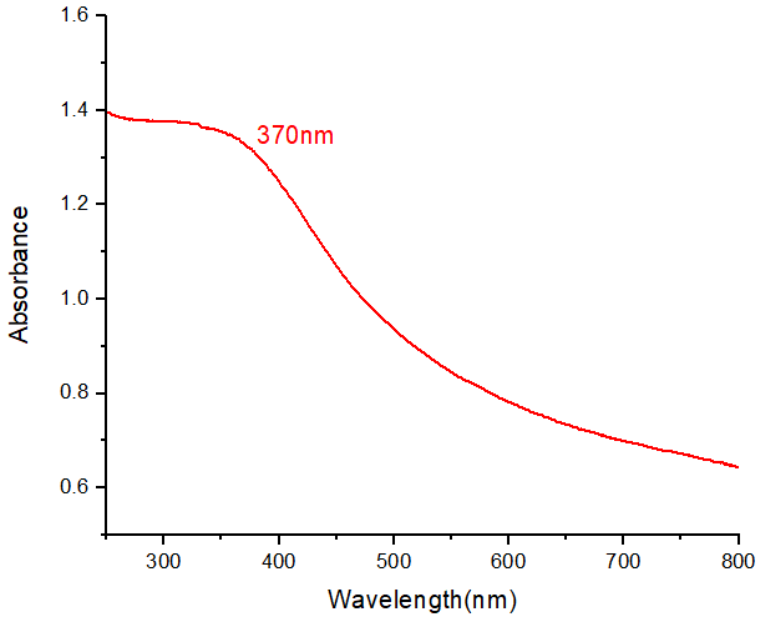

Figure 2. Uv visible spectroscopy for Dyes:.

2.3.2. FTIR

FTIR spectra of C. clementina fruits peels-assisted with ZnO nanocomposites below the wave numbers range of 4000–400 cm−1. This spectrum shows numerous functional groups[18]. FTIR transmission spectra for the prepared silver nanocomposites using plant peels Fig.3. FTIR spectra shows the shift in transmission peaks caused by the material and its impregnation. In case of carbon quantum dots, clear transmission peaks were observed at 3394,2358,2342, 1407,1083,873,711 [19].CHO stretching vibration of amine groups at 1,083 cm−1[20].The broad band at 3394.95 cm−1 was indicated the existence of stretching vibrations of –NH2 and –OH. Sharp peaks at 1401.59 cm−1 corresponds to the carbonyl group due to the presence of bioactive compounds in the form of C–O stretching The C-H (aromatic) functional group was ascribed to the bands seen at 873 cm1. The C-C stretching of aromatic rings is responsible for the absorption maxima at 1407 cm1. The spectra showed a band at around 711.9 cm1; this signal is the typical Zn-O bond signal, confirming that the substance is zinc oxide. [21]

Preprints.org (www.preprints.org) | NOT PEER-REVIEWED | Posted: 17 December 2024 doi:10.20944/preprints202412.1337.v1

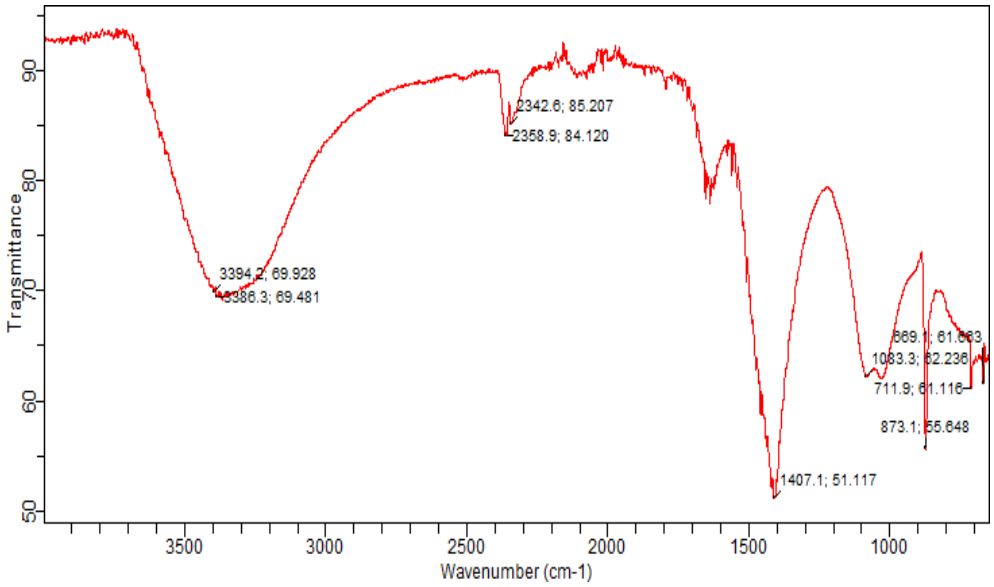

Figure 3. Ag- ZnO Nanocomposites FTIR Spectra.

2.3.3. Scaning Electron Micoscope (SEM)

Scaning electron microscope images shows the morphology of surface well, and surface morpholgies of of nanocomposites at 50000x,25000x,13000x and 4000x magnification as indicated in 4a, 4b,4c,4d respectively. SEM images clearly shows that nanocomposites are thread-like road shaped with some agglomeration also present in it.EDX spectra shows elemental composition of synthesized nanocomposites. EDX spectra of nanocopmosites shows the maximum presence of C with 45.12% because combustion process is used. In addition to this some other elements are also present like O, CL,CaZn ,Ag 19.31%,2.72%,2.93%,14.81%,15.11% respectively.

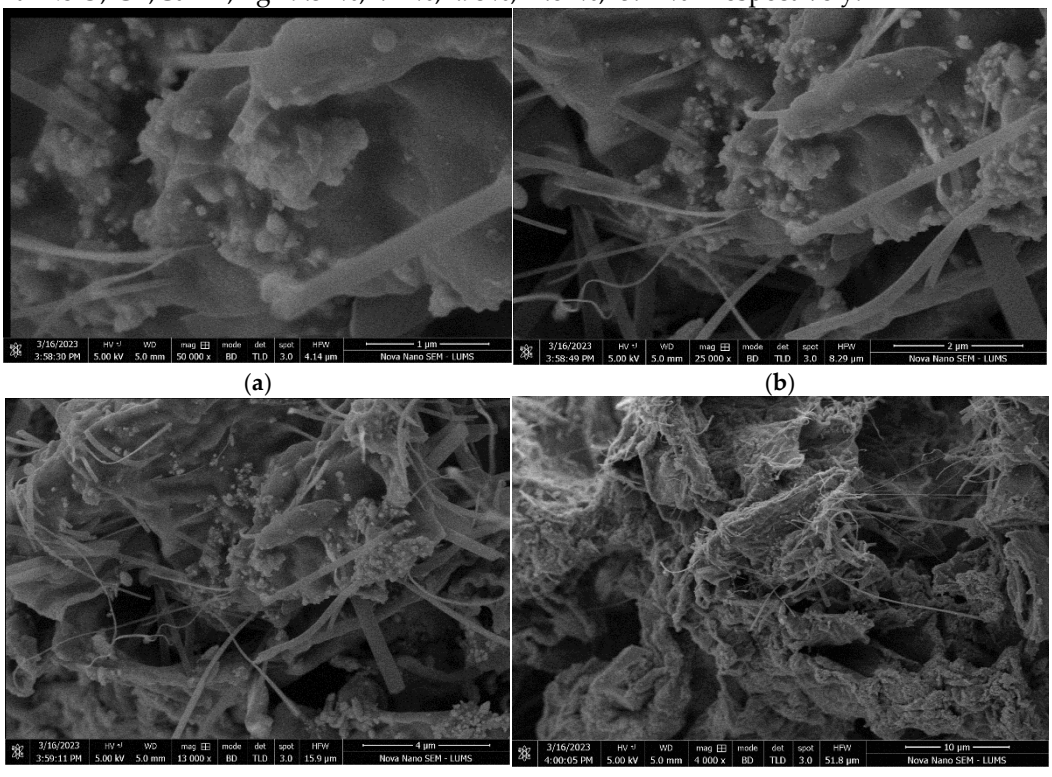

Figure 4. SEM images of Synthesized Ag-ZnO nanocomposites.

Preprints.org (www.preprints.org) | NOT PEER-REVIEWED | Posted: 17 December 2024 doi:10.20944/preprints202412.1337.v1

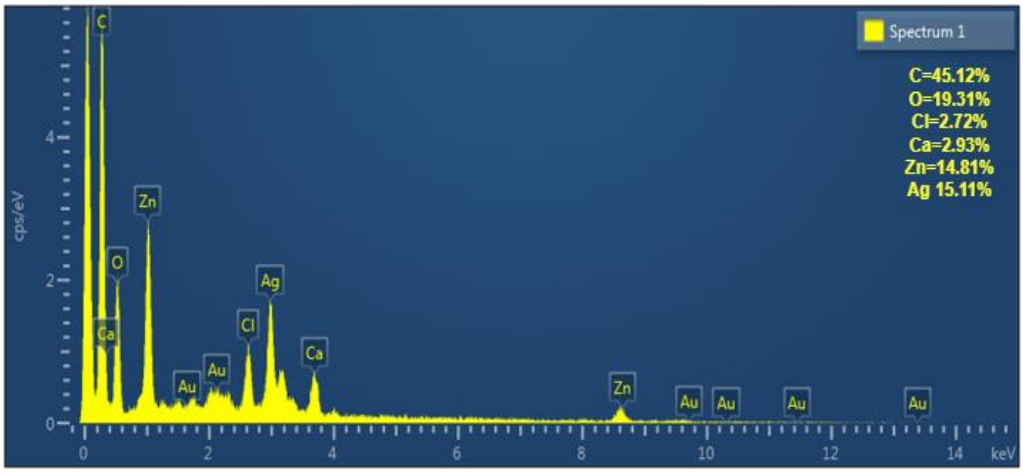

Figure 5. EDX spectra for Ag – ZnO nanocomposite.

2.3.4. X-Ray Diffraction

The crystallinity of the synthesized Ag–ZnO nanocomposites were examined by X-ray diffraction (XRD) analyzer with refection geometry at 2θ values (10°-90°). Upon doping with of Ag, Ag-ZnO nanocomposite displays four additional peaks at 38.25°, 44.36°, 64.30°, and 77.34°, which correspond to the (111), (200), (220), and (311) planes, respectively These peaks demonstrated that Ag-ZnO nanocomposites have a face centre cubic (fcc) structure. As the amount of Ag increase, the peak's strength progressively rises, indicating that Ag nanocomposites have successfully formed on the ZnO surface. While the strength of the Ag peak rises with increasing Ag concentration, the peak intensity of ZnO falls, suggesting a reduction in crystallinity and particle size in Ag-ZnO[22].

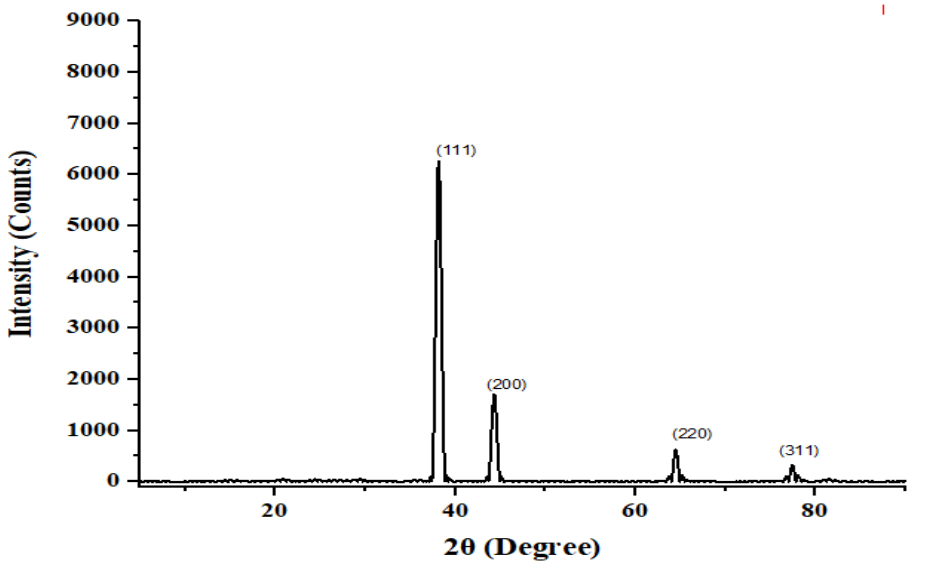

Figure 6. XRD Spectra of Ag-ZnO Nanocomposites.

2.3.5. Adsorption Studies

The mass transfer method known as adsorption includes the buildup of materials at the interface between two phases, such as a liquid-liquid, gas-liquid, gas-solid, or liquid-solid contact. The material being adsorbed is known as the adsorbent, and the substance being adsorbed is known as the adsorbate.[23]. With the use of aqueous solutions, colours were adsorbed onto nanocomposites in a batch procedure.The variable factors, such as contact duration, starting dye concentration,

 doi:10.20944/preprints202412.1337.v1

medium pH, and temperature, were examined. Except for the first concentration experiment, each experiment involved adding 40 mg of Ag-ZnO nanocomposites to 20 ml of dye solution. On an orbital shaker, the liquid was agitated at 150 rpm for 60 minutes after being poured into a 250 ml conical flask. The amount of dyes that were adsorbed was calculated using a spectrophotometric technique at 517 nm and 498 nm for the dyes, respectively, and the concentration change of the dyes in solution following adsorption.[24].

2.3.6. Kinetic Studies

For kinetic studies, 150ml volumetric flasks containing 20ml of each dye solution were used. These flasks contained 40 mg of properly weighted ZnO nanocomposites, and adsorption tests were carried out there at various temperatures, with the ideal beginning dye concentration and PH. Following 60 minutes of shaking, these solutions were filtered, and the quantity adsorbed over the adsorbent was calculated by spectrophotometric analysis. [25].

The quantity of material adsorbed over the adsorbent was calculated using the method below,

$$\%age\ Removal = C_{ads}/C_o*100$$

Where Ce is the dye's initial concentration and Cads is the quantity of dye that has been absorbed onto the surface of the adsorbent.

2.3.7. Adsorption Isotherm

Adsorption isotherms are basics to identify the nature of the interaction between adsorbate and the adsorbent used for the removal of pollutants. In beakers with 20 ml of each dye solution at a different starting concentration ranging from 100 to 600 ppm, 40 mg of nanocomposites were added. On the orbital shaker, all of the solutions were shaken for 60 minutes. Calculations were made of the quantity of dye adsorbed at time interval qt (mg/g) and equilibrium qe (mg/g). by following equation

$$(C_o\text{-}C).\ v/m = q$$

To analyse the adsorption experiments, the Langmuir, Freundlich, Temkin, Halsey, and Harkin's Jura adsorption isotherm models were used. In these models, Co represents the dye's initial concentration, C represents the solution's initial concentration following contact, V represents the treated solution's volume, and m represents the mass of the adsorbent material. (jute-stick-powder).

3. Results and Discussions

The studies in this work were conducted using simulated synthetic aqueous solutions (SSAS) of various dye concentrations to prevent interference from other components in wastewater. By dissolving known weights of the dyes Eosin Y and Congo-Red in one liter of distilled water, a 1000 ppm stock solution of the dyes was created. By diluting the stock solution with distilled water to the required concentrations for the experimental work, all solutions used in the studies were created. A UV–visible spectrophotometer was used to detect the dye concentrations.

3.1. Optimization of Parameters for Dyes

3.1.1. Dosage Effect

Establishing the optimal adsorbent dosage that reduces hazardous compounds to the bare minimum is crucial. By holding the other parameters constant, the effect of the dose parameter on the removal of organic pollutants (dyes) was examined. Figure illustrates how ZnO nanocomposites (green) can effectively remove dyes from waste water, such as Eosin Y and Congo-Red, when the dosage of the adsorbent is increased from 0.01g to 0.09g and from 0.02g to o.1g for the corresponding dyes, respectively. Other variables, such as time, concentration, and temperature, remained the same. The findings indicated that dye removal significantly increased with increasing adsorbent dosage.

 doi:10.20944/preprints202412.1337.v1

The maximal dose of congo-Red and ZnO nanocomposites for Eosin Y was 0.06g and 0.05g, respectively. For Eosin Y and Congo-Red, the ideal elimination percentages were 81% and 84%, respectively. The statistics on the adsorbent's impact are shown as a function of time and % removal.[26].

3.1.2. Concentration Effect

ZnO nanocomposites' ability to remove dyes was assessed using varying concentrations (initial). Only the concentration was altered; the other variables, including time, adsorbent dose, PH, temperature, and periods (30 minutes), were constant. Optimum concentration for Eosin Y and congo-Red was 500ppm and 600ppm respectively. Optimum percentage removal was 84% and 87% respectively.(Aravindhan, Fathima et al. 2007).

3.1.3. Time Effect

For kinetic study, dyes removal for ZnO nanocomposites was evaluated at 50 ppm and 60 ppm in different time intervals such as 10,20,30,40,50,60,70,80, and 90 minutes with optimum dosage and concentration of each adsorbent respectively. The removal of dyes was increased with the increase in contact time from 10 to 60 minutes and after which there is no any significant changes in the removal of dye. Initially, the presence of more active sites contributed to the dyes being removed quickly. Maximum of percentage removal of Eosin Y was88% observed at 50 minutes. Optimum removal of Congored was 87.2% at 60 Minutes[27].

3.1.4. PH Effect

In order to determine the influence of PH on the dye adsorption of nanocomposites, experiments were conducted at the optimum concentration and dosage. PH were retained at 2,4,6,8,10,12 and 14 PH to test the impact of dye adsorption by adding 0.1 Molar sodium hydroxide (NaOH) and 0.1 molar hydrochloric acid (HCL) to maintain PH The amount of adsorption is significantly influenced by the pH of the dye solution since it affects the stability, colour intensity, and extent of the dye. [28].

3.1.5. Temperature

To determine the impact of temperature onto dye adsorption experiment were run at optimum concentration and dosage. To investigate the effect of temperature on dye removal from water, different temperature (10°, 20°, 30°, 40°,50°,60°, 70°,80°,90°) were maintained using temperature-controlled orbital shaker The ability of adsorption of both dyes increases as temperature rises, indicating that the process is endothermic. Eosin Y and Congo red dyes both showed maximum removal of ---- and ----- at temperature of 343k respectively[24].

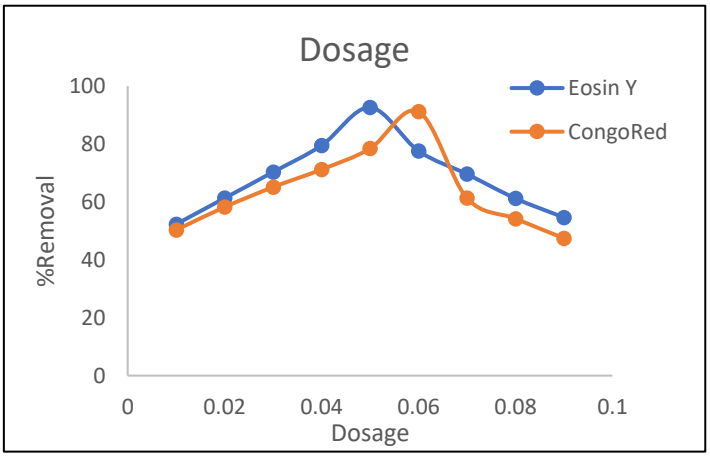

Figure 7. Dosage Effect of Green synthesized NC's for dyes Removal.

Preprints.org (www.preprints.org) | NOT PEER-REVIEWED | Posted: 17 December 2024 doi:10.20944/preprints202412.1337.v1

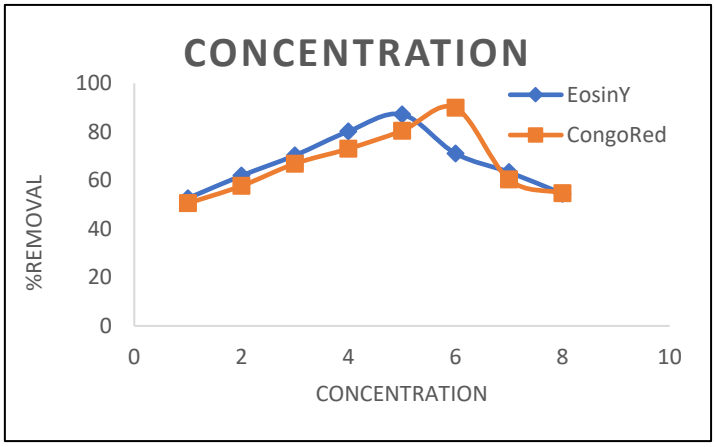

Figure 8. Concentration effect of NC's for the Removal of dyes.

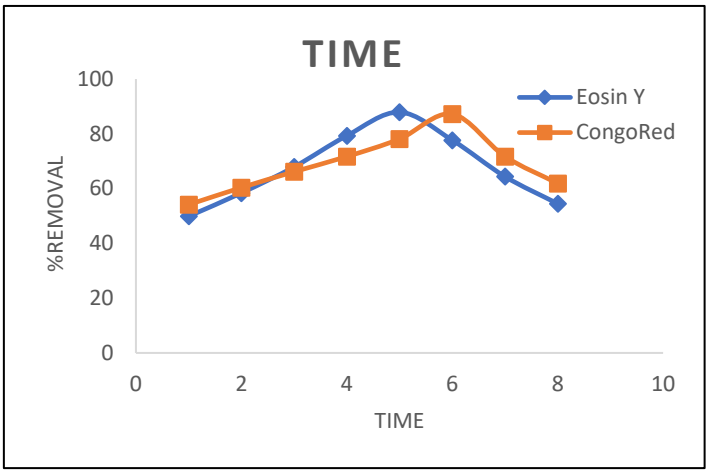

Figure 9. Optimization of Time of NC's for the Removal of Dyes.

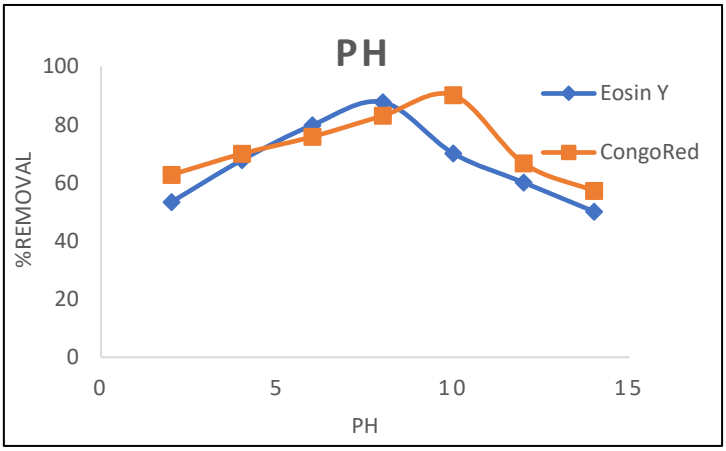

Figure 10. PH effect of NC's for the removal of Dyes.

Preprints.org (www.preprints.org) | NOT PEER-REVIEWED | Posted: 17 December 2024 doi:10.20944/preprints202412.1337.v1

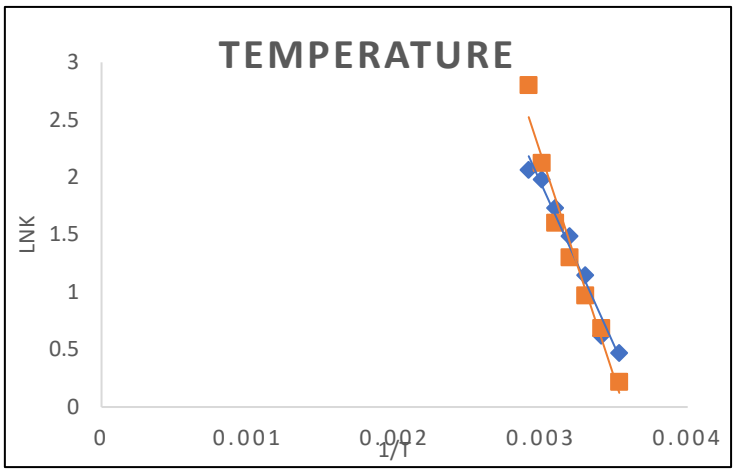

Figure 11. Optimization of Temperature for dyes Removal.

3.2. Kinetic Models

Mechanism of adsorption is clearly explained through kinetic models, which are useful for learning about equilibrium adsorption. Neutral PH and room temperature were used for experiment in this study. Lagergren's pseudo-1st -order model and Ho's pseudo-2nd-order model are the most frequently utilized kinetic models for monitoring the kinetics of adsorption processes.

Pseudo- first order: Psuedo first order models suggest a proportional relation for rate of adsorption. Linear form of first order model is as follows:

$$\ln (q_e - q_t) = \ln q_e - k_1 t$$

Where the pseudo-first adsorption model capacity rate constant is k1(1/min). Nanocomposites' adsorption capacities at equilibrium and at time t (min) are units qe and qt (mg/g).

Pseudo-2nd order: The pseudo-second order model predicts a quadratic connection for the rate of adsorption. The pseudo-second order model has the following linear form:

$$\frac{t}{qt} = \frac{1}{k2} qe^2 + \frac{t}{qe}$$

The slop and intercept of plots of t/Qt vs t used to determine the values of Qe and k2, where k2 (g/mg.min) is the constant of PSO. Below is a graphical illustration of PFO and PSO[29].

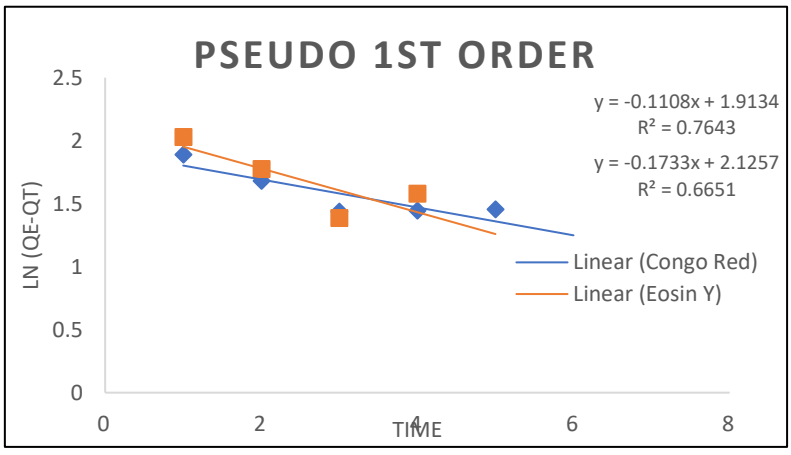

Figure 12. Pseudo 1st Order for Eosin Y and Congo- Red.

Preprints.org (www.preprints.org) | NOT PEER-REVIEWED | Posted: 17 December 2024 doi:10.20944/preprints202412.1337.v1

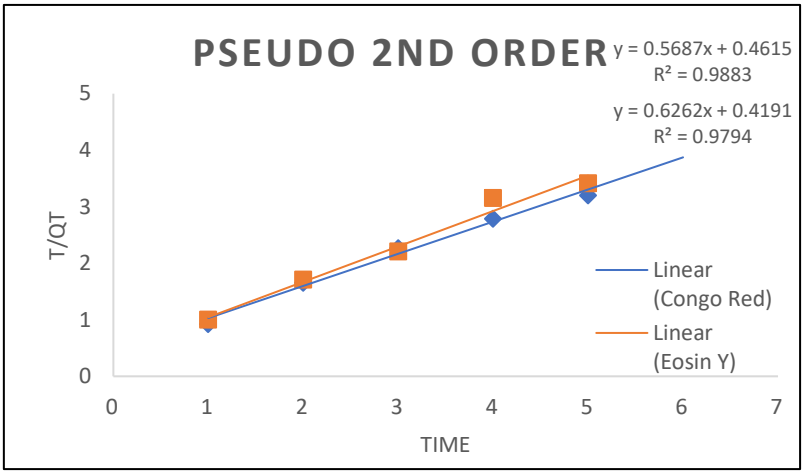

Figure 13. Pseudo Second Order for Eosin Y and Congo-Red.

Table 1. Kinetic Models of Ag/ZnO Nanocomposites for Eosin Y and Congored.

Nanocomposites		
Pseudo Second Order		
System	**Eosin Y**	**Congo-Red**
Qe($\boldsymbol{m\ mol^{-1}}$	15.969	17.583
$K^2(\boldsymbol{gm\ mol^{-1}})$	0.9357	0.7009
R^2	0.9794	0.9884
Pseudo First Order		
Qe cal($\boldsymbol{m\ mol^{g-1}}$)	8.3787	6.7760
K1 $\boldsymbol{min^{-1}}$	-0.1733	-0.1108
R^2	0.6651	0.76430

3.2.1. Adsorption of Thermodynamics

Vont Hoff equation and Gibb's free energy were used to compute change in Gibb's free energy (ΔG°), entropy (ΔS°) and enthalpy (ΔH°) linked with sorption of these dyes onto the adsorbent. Results are listed in table below.

$$Lnkc = \Delta S°/R - \Delta H°/RT$$

$$Kc = /Ce$$

$$\Delta G = \Delta H° - T\Delta S$$

Where T is the overall temperature and Kc is the adsorption (K) dispersal coefficient. R (8.314 kj mol/K) is the universal constant. Ce (in mg/L) stands for equilibrium solution concentration.

Table 2. Adsorption Thermodynamics of Ag/ZnO nanocomposites for Eosin Y & Congored.

		Eosin Y		
Temperature	**ΔG°,kl/mol**	**ΔH°,KJ/mol**	**ΔS°,J/mol.k**	**R^2**
283	-8.7080	-0.00249	0.03076	0.9756
293	-9.0157	-0.00249	0.03076	0.9756
303	-9.3208	-0.00249	0.03076	0.9756
313	-9.6284	-0.00249	0.03076	0.9756
323	-9.9360	-0.00249	0.03076	0.9756
333	-10.243	-0.00249	0.03076	0.9756
343	-10.551			
		Cono-Red		

 doi:10.20944/preprints202412.1337.v1

283	-8.4719	-0.00166	0.02993	0.9636
293	-8.7529	-0.00166	0.02993	0.9636
303	-9.0705	-0.00166	0.02993	0.9636
313	-0.9369	-0.00166	0.02993	0.9636
323	-9.6691	-0.00166	0.02993	0.9636
333	-9.9684	-0.00166	0.02993	0.9636
343	-10.267	-0.00166	0.02993	0.9636

Negative values of enthalpy (ΔH°) shows that the reaction is exothermic in case of both dyes Eosin Y and congo-Red. While the values of entropy (ΔS°) is the indicative of increased volatility on adsorbate and adsorbent surface.

3.2.2. Adsorption Isotherm

Using isotherm models, the efficiency of adsorbents in removing dyes was evaluated. Adsorption isotherm models include mechanistic details for the adsorption procedure, that are crucial for adsorption system design. To describe the adsorption of gases and solutes, isotherms or the quantity of adsorbates on the adsorbents as a function of the adsorbate's pressure (if it's a gas) or concentration (if it's a liquid phase solute—are frequently utilised. The equilibrium data were evaluated using models by Langmuir, Temkin Halsey, Freundlich, and Harkins models[30].

3.2.3. Langmuir Isotherm

Using Langmuir adsorption, which was first developed to describe solid-gas phase adsorption, the adsorption capacity of various adsorbents is measured and compared. The Langmuir isotherm describes the surface coverage by achieving dynamic equilibrium between the adsorption and desorption rates. Surface area of the adsorbent has an inverse relationship with adsorption[31].

$$\frac{Ce}{qe} = \frac{1}{qmKe} + \frac{Ce}{qe}$$

3.2.4. Frendlich Isotherm

The earliest known connection explaining the adsorption equilibrium is the Freundlich adsorption isotherm based on adsorption on a heterogeneous surface.

$$\text{Log qe} = \log K_f + \frac{1}{n} \log \text{Ce}$$

Ce stands for the equilibrium concentration (mg/L), qe for the quantity of adsorbate (in mg/g), and KF and 1/n for empirical constant that, respectively, represent the adsorption capacity and intensity[32].

3.2.5. Temkin Isotherm

While ignoring extremely low and extremely high concentration values, the Temkin models, which assume a multilayer adsorption process, takes into consideration interactions between the adsorbents and the adsorbates.

$$\text{qe} = \frac{RT}{b} \ln (\text{Km Ce})$$

where t is the temperature in k, Km is the Temkin isotherm constant in L/g, R is the Temkin constant connected to sorption heat in J/mol, T is the universal gas constant in J/(mol K), and R is the Temkin constant[33].

Preprints.org (www.preprints.org) | NOT PEER-REVIEWED | Posted: 17 December 2024 doi:10.20944/preprints202412.1337.v1

3.2.6. Harkins-Jura Isotherm

The main characteristics of the Harkins-jura isotherm model are multi-layer adsorption and the presence of heterogeneous pore distribution on adsorbent surfaces.

$$\left[\frac{1}{qe2}\right] = \left[\frac{BHJ}{AHJ}\right] - \left[\frac{1}{AHJ}\right] \log (Ce)$$

where the Harkins-Jura constants are BHJ and Ahj. The slope and the intercept of the linear plot created on 1/qe2 vs log Ce may be impelied to calculate both Bhj and Ahj [34].

3.2.7. Halsey Isotherm

Using the Halsey isotherm model, the multi-layer adsorption system for metallic ions adsorption at a comparatively wide distance from the surface may be assessed.

$$\text{Ln(qe)}=\left[\left(\frac{1}{nh}\right)\ln\ (\text{KH})\right] - \left(\frac{1}{nh}\right)\ln(1/\text{Ce})$$

The Halsey isotherm model may be used to assess the multilayer adsorption system for metal ions adsorption at a comparatively considerable distance from the surface.)[34].

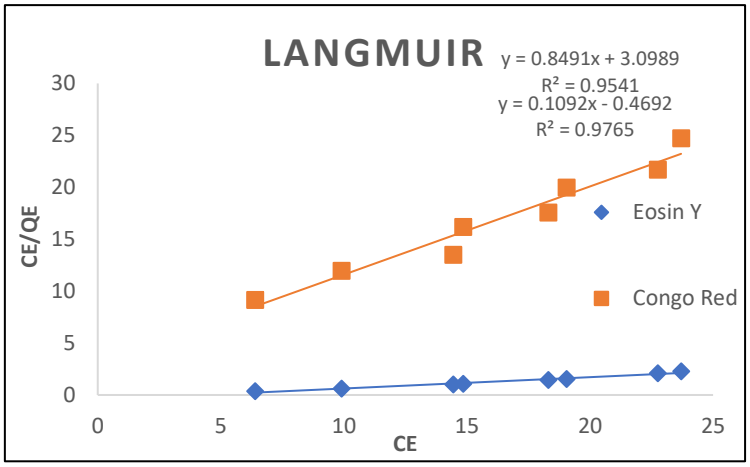

Figure 14. Langmuir Isotherm for Dyes.

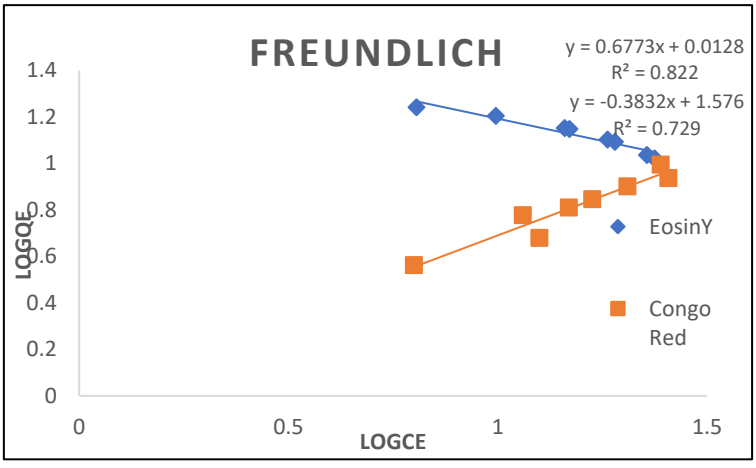

Figure 15. Freundlich Isotherm for Dyes.

Preprints.org (www.preprints.org) | NOT PEER-REVIEWED | Posted: 17 December 2024 doi:10.20944/preprints202412.1337.v1

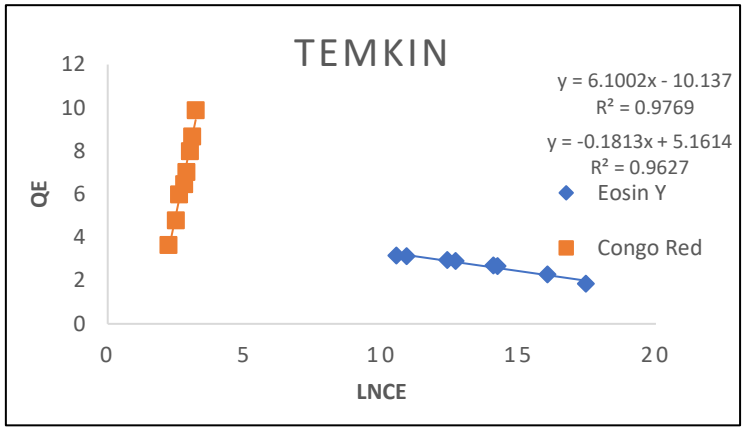

Figure 16. Temkin Isotherm for Dyes.

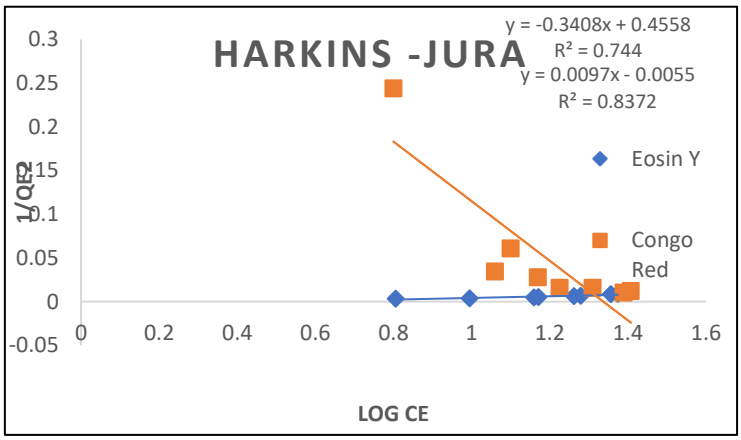

Figure 17. Harkin's Jura Isotherm for Dyes.

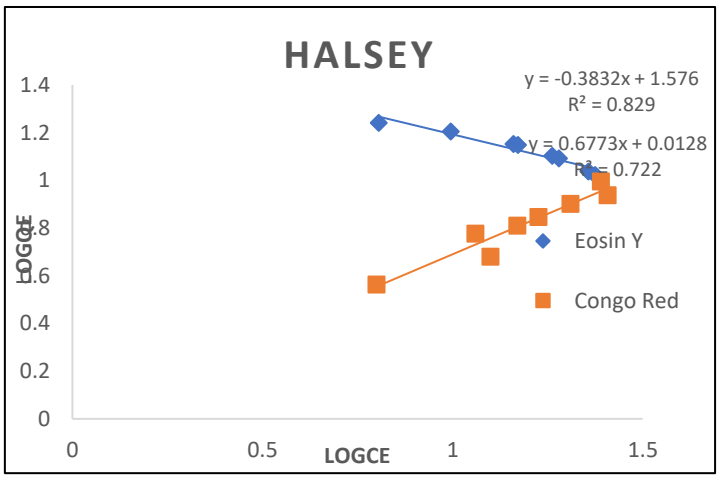

Figure 18. Halsey Isotherm for Dyes.

Table 3. Adsorption isotherm for Eosin Y and Congored by Ag/ZnO nanocomposites.

System	Eosin Y	Congo-Red
Langmuir Isotherm		
Qm(mg/g)	14.3226	13.0153
Kl (L/mg)	3.6509	4.5440
RL	0.01351	0.0111
R2	0.9541	0.9765

 doi:10.20944/preprints202412.1337.v1

Frendlich		
K (L/mg)	0.0347	4.2840
N	1.476	-2.609
R2	0.712	0.801
Temkin		
B(mg/L)	16.002	15.183
α(L/mg)	11.565	12.48
R2	0.9769	0.9627
Harkins-jura		
B	-1.338	103.09
A	-2.936	-0.567
R2	0.744	0.872
Halsey		
Nh	-2.617	1.4764
KH	-1.4067	0.0511
R2	0.829	0.722

3.3. Regeneration Studies

Reusability of the nanocomposites in the EY and CR removal was investigated for 5 successive cycles. After each run, the adsorbent was centrifuged to separate it, then it was repeatedly rinsed with distilled water to aid in desorption before being dried for six hours at 1000°C. The recycled solid was used for the next run. The removal efficiency of EY and CR for the 1st time was 85.91% and 70.02% and then decreases to 31 % and 50.3% respectively in the fifth cycle. The results showed that both dyes have less reusability capacity after fifth adsorption-desorption cycles. The maximum adsorption capacity of the Eosin Y and Congo-Red from aqueous solution was 144.25mg/g and 147.3mg/g respectively.

3.4. Point of Zero Charge (PZC) Determination

10ppm dilute solution of Eosin Y and Congo- Red dyes was prepared in 200ml distilled water. Then 20ml solution of each dye was taken in 20 different beakers and the beakers was tagged with the names of dyes. Then, using PH paper and either 0.1M NaOH or 0.1M HCL solutions, various PH values ranging from 3 to 12 were set for both colours. Then in each beaker added the equal amount of Composite i.e. 0.02g in Eosin Y dye containing beakers while 0.04g in Congo-red dye containing beakers. Then the beakers were set on the shaker and shaked the flasks at speed 150rpm on an orbital shaker for 1 hour. After equilibrium, all the solutions ware filtered and PH values were recorded accordingly. Then the graph was plotted between Initial PH Values and change in PH values as shown in the graphs given below.

Preprints.org (www.preprints.org) | NOT PEER-REVIEWED | Posted: 17 December 2024 doi:10.20944/preprints202412.1337.v1

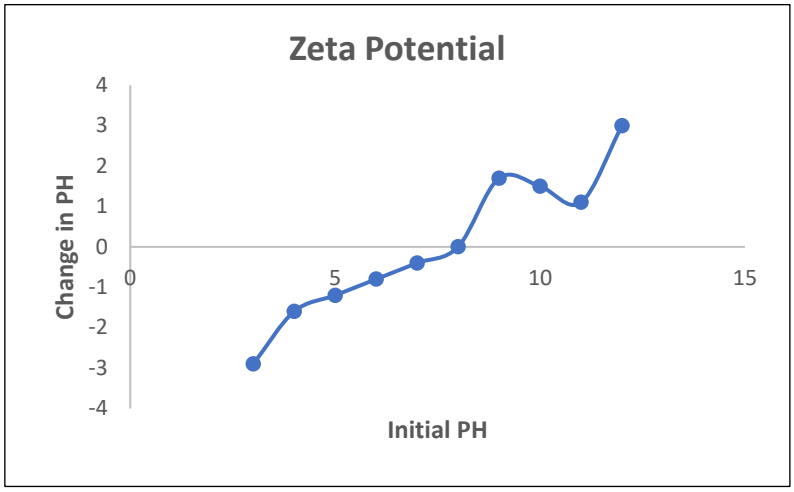

Figure 19. The line intersects the Phi axis at 8 which is the zeta potential value of ZnO nanocomposites with Eosin Y dye.

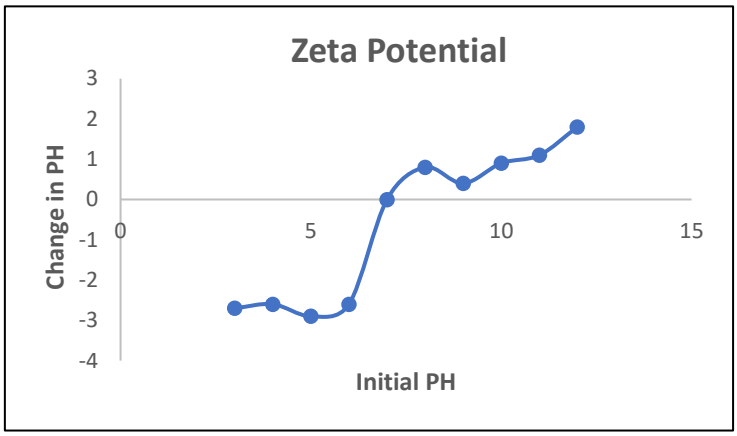

Figure 20. The line intersects the Phi axis at 7 which is the zeta potential value of ZnO nanocomposites with Congo-red dye.

4. Conclusions

This study has been designed to improve the adsorption capability of Ag doped ZnO nanocomposites as adsorbent materials for the cost-effective and efficient removal of dyes from contaminated water. Fourier Transform Infrared spectroscopy(FTIR), UV-Visible spectroscopy, X-ray Diffraction and Scanning Electron Microscopy have been used to characterize the prepared ZnO nanocomposites. The adsorption capacity of ZnO nanocomposites was calculated for the removal of two dyes (Eosin Y and Congo-Red). Different parameters i.e., Dosage, Concentration, Time, PH and temperature have been studied. The results showed that maximum removal of Eosin Y was at 0.05g dosage at 500ppm concentration in 50 minutes, while maximum removal of Congo-red was at 0.06g dosage at 300ppm concentration in 60 minutes. The reaction between dyes and adsorbent is exothermic and spontaneous. Positive values of entropy showed that there is increase in randomness at adsorbates and adsorbents surfaces. Kinetic studies showed that Pseudo 2nd order model is best fitted. The Linear isotherms i.e. Langmuir and Temkin are best fitted adsorption isotherms, Langmuir with R^2= 0.9541 for eosin y dye and R2 = 0.9765 for congo-Red dye and for temkin Eosin Y R2 = 0.9769 and Congo-Red R2= 0.9627 for the removal of dyes. The Nanocomposites prepared from *Citrus Celementine* peels may be used as an efficient adsorbent material for the effective removal of dyes from wastewater.

 doi:10.20944/preprints202412.1337.v1

Funding: No funding taken from any organization.

Conflicts of Interest: Authors declare no conflict of interest among themselves.

References

1. Bhattacharya, D. and R.K. Gupta, *Nanotechnology and potential of microorganisms.* Critical reviews in biotechnology, 2005. **25**(4): p. 199-204.
2. Logothetidis, S., *Nanomedicine: the medicine of tomorrow*, in *Nanomedicine and Nanobiotechnology*. 2011, Springer. p. 1-26.
3. Shao, G.N., H. Kim, and S. Imran, *https://www. sciencedirect. com/science/article/abs/pii/S092633731500346X.* 2016.
4. Naseem, T. and M. Waseem, *A comprehensive review on the role of some important nanocomposites for antimicrobial and wastewater applications.* International Journal of Environmental Science and Technology, 2022: p. 1-26.
5. Nasrollahzadeh, M., et al., *An introduction to nanotechnology*, in *Interface science and technology*. 2019, Elsevier. p. 1-27.
6. Molla, M.A.I., et al., *Fabrication of Ag-doped ZnO by mechanochemical combustion method and their application into photocatalytic Famotidine degradation.* Journal of Environmental Science and Health, Part A, 2019. **54**(9): p. 914-923.
7. Shao, X.L., et al., *A study of the transition between the non-polar and bipolar resistance switching mechanisms in the TiN/TiO 2/Al memory.* Nanoscale, 2016. **8**(36): p. 16455-16466.
8. Chaudhry, F.N. and M. Malik, *Factors affecting water pollution: a review.* J. Ecosyst. Ecography, 2017. **7**(1): p. 225-231.
9. Singh, S., K.L. Wasewar, and S.K. Kansal, *Low-cost adsorbents for removal of inorganic impurities from wastewater*, in *Inorganic pollutants in water*. 2020, Elsevier. p. 173-203.
10. Ali, I. and V. Gupta, *Advances in water treatment by adsorption technology.* Nature protocols, 2006. **1**(6): p. 2661-2667.
11. Du, X., et al., *Approaching ballistic transport in suspended graphene.* Nature nanotechnology, 2008. **3**(8): p. 491-495.
12. Harja, M., G. Buema, and D. Bucur, *Recent advances in removal of Congo Red dye by adsorption using an industrial waste.* Scientific Reports, 2022. **12**(1): p. 6087.
13. Liu, Y., et al., *Adsorption of toxic dye Eosin Y from aqueous solution by clay/carbon composite derived from spent bleaching earth.* Water Environment Research, 2021. **93**(1): p. 159-169.
14. Rashed, M.N., *Adsorption technique for the removal of organic pollutants from water and wastewater.* Organic pollutants-monitoring, risk and treatment, 2013. **7**: p. 167-194.
15. Rashid, R., et al., *A state-of-the-art review on wastewater treatment techniques: the effectiveness of adsorption method.* Environmental Science and Pollution Research, 2021. **28**: p. 9050-9066.
16. Zhang, Z., et al., *Green synthesis of fluorescent nitrogen–sulfur Co-doped carbon dots from scallion leaves for hemin sensing.* Analytical Letters, 2020. **53**(11): p. 1704-1718.
17. Suresh, D., et al., *Green synthesis of multifunctional zinc oxide (ZnO) nanoparticles using Cassia fistula plant extract and their photodegradative, antioxidant and antibacterial activities.* Materials Science in Semiconductor Processing, 2015. **31**: p. 446-454.
18. Anuradha, C. and P. Raji, *Citrus limon fruit juice-assisted biomimetic synthesis, characterization and antimicrobial activity of cobalt oxide (Co 3 O 4) nanoparticles.* Applied Physics A, 2021. **127**: p. 1-9.
19. Zhu, J., et al., *Green preparation of carbon dots from plum as a ratiometric fluorescent probe for detection of doxorubicin.* Optical Materials, 2021. **114**: p. 110941.
20. Karthiga Devi, G., P. Senthil Kumar, and K. Sathish Kumar, *Green synthesis of novel silver nanocomposite hydrogel based on sodium alginate as an efficient biosorbent for the dye wastewater treatment: prediction of isotherm and kinetic parameters.* Desalination and Water Treatment, 2016. **57**(57): p. 27686-27699.
21. Luque, P., et al., *Green synthesis of zinc oxide nanoparticles using Citrus sinensis extract.* Journal of Materials Science: Materials in Electronics, 2018. **29**: p. 9764-9770.
22. Mtavangu, S.G., et al., *In situ facile green synthesis of Ag–ZnO nanocomposites using Tetradenia riperia leaf extract and its antimicrobial efficacy on water disinfection.* Scientific Reports, 2022. **12**(1): p. 15359.
23. Grassi, M., et al., *Removal of emerging contaminants from water and wastewater by adsorption process.* Emerging compounds removal from wastewater: natural and solar based treatments, 2012: p. 15-37.
24. Du, W.L., et al., *Preparation, characterization and adsorption properties of chitosan nanoparticles for eosin Y as a model anionic dye.* Journal of hazardous materials, 2008. **153**(1-2): p. 152-156.
25. Mittal, A., et al., *Adsorptive removal of hazardous anionic dye "Congo red" from wastewater using waste materials and recovery by desorption.* Journal of colloid and interface science, 2009. **340**(1): p. 16-26.
26. Kalotra, S. and R. Mehta, *Synthesis of polyaniline/clay nanocomposites by in situ polymerization and its application for the removal of Acid Green 25 dye from wastewater.* Polymer Bulletin, 2021. **78**: p. 2439-2463.

 doi:10.20944/preprints202412.1337.v1

27. Anitha, T., *Synthesis of nano-sized chitosan blended polyvinyl alcohol for the removal of Eosin Yellow dye from aqueous solution.* Journal of Water Process Engineering, 2016. **13**: p. 127-136.
28. Mahmood, K., et al., *Green synthesis of Ag@ CdO nanocomposite and their application towards brilliant green dye degradation from wastewater.* Journal of Nanostructure in Chemistry, 2021: p. 1-13.
29. Guo, X. and J. Wang, *A general kinetic model for adsorption: Theoretical analysis and modeling.* Journal of Molecular Liquids, 2019. **288**: p. 111100.
30. Wang, J. and X. Guo, *Adsorption isotherm models: Classification, physical meaning, application and solving method.* Chemosphere, 2020. **258**: p. 127279.
31. Ayawei, N., A.N. Ebelegi, and D. Wankasi, *Modelling and interpretation of adsorption isotherms.* Journal of chemistry, 2017. **2017**.
32. Alagumuthu, G., V. Veeraputhiran, and R. Venkataraman, *Adsorption isotherms on fluoride removal: batch techniques.* Arch. Appl. Sci. Res, 2010. **2**(4): p. 170-185.
33. Kalam, S., et al., *Surfactant adsorption isotherms: A review.* ACS omega, 2021. **6**(48): p. 32342-32348.
34. Liu, J. and X. Wang, *Novel silica-based hybrid adsorbents: lead (II) adsorption isotherms.* The Scientific World Journal, 2013. **2013**.